

The topology and polarization of sub-beams associated with the ‘drifting’ subpulse emission of pulsar B0943 + 10 – III. Analysis of Pushchino 103/40-MHz observations

Joanna M. Rankin,¹*† Svetlana A. Suleymanova²* and Avinash A. Deshpande³*‡

¹*Sterrekundig ‘Anton Pannekoek’, University of Amsterdam, NL1098, Netherlands*

²*Pushchino Radio Astronomy Observatory, Lebedev Physical Institute, Moscow 117924, Russia*

³*Raman Research Institute, Bangalore 560 080, India*

Accepted 2003 January 3. Received 2002 December 5; in original form 2002 March 22

ABSTRACT

The rotating emission-beam system of pulsar B0943 + 10 was explored in Paper I of this series using Arecibo observations at 430 and 111 MHz and in Paper II using Gauribidanur 35-MHz data. Here, we have the opportunity to study simultaneous, dual-frequency observations carried out at the Pushchino Radio Astronomy Observatory some 10 yr ago at frequencies of 103 and 40 MHz. The apparent modulation periods (P_3) and circulation times derived from the 11 d of observations seem to fall into two distinct ranges, apparently correlated with profile modal effects. The 103-MHz maps bear a strong resemblance to the 111-MHz Arecibo sequence studied in Paper I, but show a variety of sub-beam intensity patterns, whereas similar comments can be made about the 40-MHz maps in relation to the 35-MHz maps of Paper II. Most interesting here is the result that there is little correspondence between the sub-beam maps at the two frequencies. Only for two of the observations do we find a correspondence between the pairs: one of the ‘B’-mode sequences with an asymmetric pattern as well as a ‘Q’-mode sequence occurring immediately prior to a transition to the ‘B’ mode. Finally, we find that our various ‘B’-mode observations vary markedly in their profile linear polarization. The strongest sequences suggest differing proportions of secondary polarization mode power.

Key words: MHD – plasmas – polarization – radiation mechanisms: non-thermal – pulsars: general – pulsars: individual: B0943 + 10.

1 INTRODUCTION

In this paper we continue our study of the emission-beam pattern of pulsar B0943 + 10, making use of its remarkably stable ‘drifting’ subpulse sequences. While the potential of this situation was outlined in Deshpande & Rankin (1999) (see also Deshpande 2000; Rankin & Deshpande 2000), Papers I and II of this series [Deshpande & Rankin (2001) and Asgekar & Deshpande (2001), respectively] have given detailed analyses of the star’s subpulse modulation, using Arecibo observations at 430 and 111.5 MHz, and 35-MHz observations from the Gauribidanur Observatory.

These two programmes of analysis have begun to reveal the character and dynamics of the pulsar’s emission-beam system. Obser-

vations separated by many years and over a broad frequency range have shown that its ‘B’-mode pulse sequences are produced by a pattern of just 20 sub-beams which rotate anticlockwise around the pulsar’s ‘nearer’ magnetic axis in an interval of about 37 pulsar rotation periods (P_1) or some 41 s. The striking circumstance that the pulsar’s (‘B’-mode) radiation consists of a vigesimal beam system over the full 35–430 MHz range of the observations strongly suggests that the radiation is produced within a system of emission columns, which, being ‘seeded’ in the acceleration region, rise up through the emission region and extend out well beyond it. A marked difference, however, between the 35-MHz observations and those at higher frequencies is that some individual sub-beams (or a group of them) are more frequently weak or missing – though the vigesimal nature of the overall system is still strongly maintained – raising immediate questions about how the low- and high-frequency patterns correspond.

Moreover, the star’s ‘Q’-mode behaviour stands in fascinating contrast to that of the ‘B’ mode. The regular subpulse modulation – evidenced by the $0.53 c/P_1$ fluctuation feature – disappears. The subpulses appear disorganized and, while weaker overall,

*E-mail: jrankin@astro.uva.nl, Joanna.Rankin@uvm.edu (JMR); suleym@prao.psn.ru (SAS); desh@rri.res.in, desh@naic.edu (AAD)

†On leave from: Physics Department, University of Vermont, Burlington, VT 05405, USA

‡Current address: Arecibo Observatory, Box 53995, Arecibo, Puerto Rico 00612.

some are remarkably bright, indeed brighter than any usually seen in ‘B’-mode sequences. The average profile assumes a different form, and the secondary polarization mode (SPM) predominates throughout the profile. Underlying this disorganization, we found evidence in Paper I that the overall beam system continues to rotate in the ‘Q’ mode, at perhaps a slightly different rate, even though only one or two sub-beams remain active.

Here, we have the opportunity to study simultaneous, dual-frequency observations of pulsar 0943 + 10 for the first time. Section 2 discusses the observations, Section 3 our efforts to determine the primary modulation frequencies of the ‘B’-mode sequences, and Sections 4 and 5 present the sub-beam maps of the ‘B’- and ‘Q’-mode observations, respectively. Then, in Sections 6 and 7 we discuss their polarization and briefly summarize the results and conclusions.

2 OBSERVATIONS

The observations were conducted at the Pushchino Radio Astronomy Observatory (PRAO) using the BSA (Bolshaya Synfaznaya Antenna) at 103.13 MHz and the east–west arm of the DKR-1000 cylindrical paraboloid cross telescope at 39.898 MHz.¹ Most of the observations were carried out on 22 nights during 1990 December, and the 11 simultaneous pulse-sequence (PS) pairs used in this analysis were chosen for their relatively good signal-to-noise ratio (S/N) in both bands.² One could not ask for a more diverse set of observations for initial study. As summarized in Table 1, the dual-band observations on December 8, 10, 16, 17, 23, 24 and 27 are ‘B’-mode sequences, marked by the usual asymmetrical profiles; December 26 is an unusual ‘B’-mode sequence with a nearly symmetrical double profile at 103 MHz; December 7 records a transition from the ‘Q’ to the ‘B’ mode; and December 20, 22 and 28 are entirely ‘Q’-mode sequences. Also, we had available four later 103-MHz PSs, two each in the ‘B’ and ‘Q’ modes.

The signals from these linearly polarized arrays were fed to radiometers with 64×20 -kHz contiguous channels (BSA) and 32×5 -kHz channels (DKR-1000) in order to measure the total intensity and its spectral variations across the passband. The dedispersed pulses were referred to the frequency of the first channel – that is, to 103.130 and 39.898 MHz (hereafter, 103 and 40 MHz). This choice of frequencies makes the sampled windows of the two bands adjacent in time, apart from the overall dispersion delay of $31 P_1$.

By observing a partially linearly polarized pulsar signal at adjacent frequencies, the rotation measure can be obtained, which for observing frequencies of 40 and 103 MHz gives $RM = 15 \pm 1$ rad m^{-2} . The Faraday modulation period Δf is related to the frequency f by $\Delta f = 1.748 \times 10^{-5} f^3 / RM$ (f in MHz). In that the total passband exceeded (and was a multiple of) the Faraday modulation period at these frequencies, the total intensity of the dedispersed pulses provides a reasonable estimate of Stokes parameter I . The fractional linear polarization and its associated position angle (PA) χ were then determined for each sample – using a technique developed at Pushchino (Suleymanova, Volodin & Shitov 1988) – from the Faraday-rotation-induced, quasi-sinusoidal intensity modulation across the passband. The time resolutions were 6.98 ms or

$2.29 mP_1$ at both frequencies. Most of the observations comprised 400 pulse periods, although only for some 280 of these was 0943 + 10 well within the BSA’s beam at 103 MHz.

Each of the 103-MHz sequences is thus modulated by the gain of the BSA during transit of the source, limiting the usable sequence to 280 periods, as above. Within this interval, the effects of interstellar scintillation largely appear to be averaged out, suggesting that the 20-kHz channel bandwidth exceeds the decorrelation bandwidth at 103 MHz. We see a very different behaviour at 40 MHz. The gain profile of the DKR-1000 appears to be roughly constant over the 400-pulse observations; however, the pulsar intensity is highly corrugated within this interval. ‘Flares’ of 50 pulses or so are common, and for this reason we can see from the outset that it will not be easy to find sequences that are completely comparable at the two frequencies.

3 ‘B’-MODE CIRCULATION-TIME DETERMINATION

The initial stages of our analysis will be familiar to readers of Papers I and II. We have computed the usual longitude-resolved fluctuation (LRF) spectra as well as harmonic-resolved fluctuation (HRF) spectra for each ‘B’-mode sequence, resolving questions of aliasing to show that the star’s primary subpulse modulation frequency f_3 is some $0.53 c/P_1$. Examples of these spectra can be found in Figs 1 and 4 of Paper I, where a detailed description of their computation and display will be found. The argument in Paper I went on to show, in a variety of ways, that this modulation was produced by a set of just 20 circulating sub-beams, which then define a tertiary modulation period of $20/f_3$ or some $37 P_1$. The PRAO observations provide no strong, independent confirmation (‘sidebands’ or low-frequency features) of the vigesimal character of this tertiary modulation period. We have carefully examined each sequence for such features, but no fully developed and reliable signature was identified.³ None the less, the stability and 20-fold character of the tertiary modulation of 0943 + 10 have been so well established in our foregoing analyses – and the current observations are so clearly compatible with those examined earlier – that we can proceed here confidently.

These selfsame steps were followed in our analysis of the Pushchino observations, and some of the parameters and results are given in Table 1. We first computed LRF spectra for each sequence in order both to examine its average profile (so as to establish its centre) and to assess its coherence and quality. Some examples of these are given in Figs 1–4. Here, we see the distinct profiles characteristic of the ‘B’ mode at 103 and 40 MHz in Fig. 1, the unusual ‘B’-mode profiles in Fig. 3, and the distinct ‘Q’-mode profiles in Fig. 4, to which we will return in a later section. We also see here again the remarkable regularity or ‘coherence’ of the aliased $0.46c/P_1$ feature associated with the star’s ‘drift’ – even at 40 MHz, though

³Two observations with asymmetric polar-map patterns, December 23 at 40 MHz and December 27 at 103 MHz (see Figs 5 and 6), might have been expected to produce such features, just as were found in Paper II. On closer inspection, however, neither map is fully asymmetric. Such instances reiterate how unusual, or fragile, are the conditions which retain features related to the tertiary modulation period. The smooth modulation seen in the 35-MHz observations of Paper II resulted in the detectable tertiary modulation feature in the spectrum. In the absence of such smooth variation of intensities across the sub-beam sequences, the modulation power gets shared by several harmonics of the tertiary modulation frequency, reducing the possibility of detecting any of them clearly above the noise.

¹The two instruments are fully described on the Pushchino Observatory website at <http://www.prao.psn.ru>

²Several of these sequences were analysed earlier in Suleymanova et al. (1998), but no use could then be made of their simultaneous character.

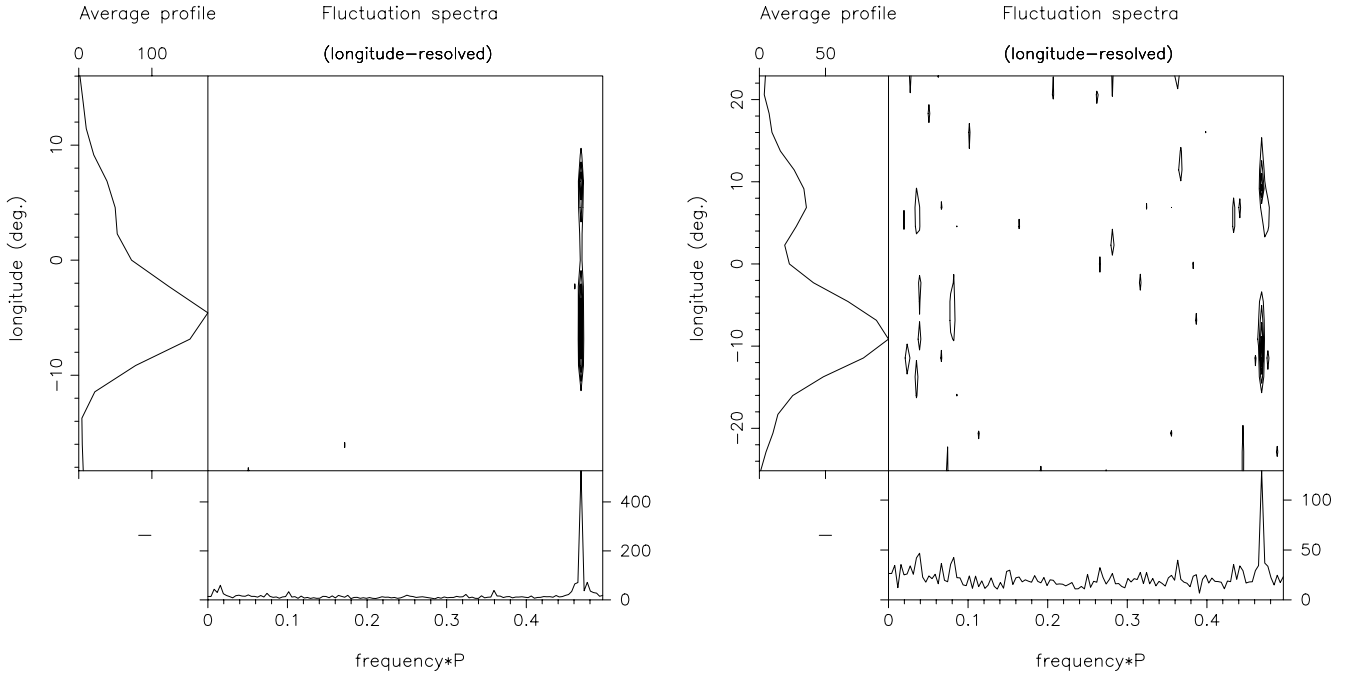


Figure 1. Characteristic ‘B’-mode profiles and LRF spectra for pulsar B0943 + 10 on 1990 December 23 at 103 (left) and 40 MHz (right). FFTs of length 256 were used. The body of the figures gives the amplitudes of the features as a set of contours. The average profiles (Stokes I) are plotted in the respective left-hand panels, and the integral spectra are given at the bottom of each figure. The pulse-sequence amplitudes were adjusted before analysis to remove any slow secular changes, so that any small $1/f$ ‘tails’ in the spectra have been suppressed.

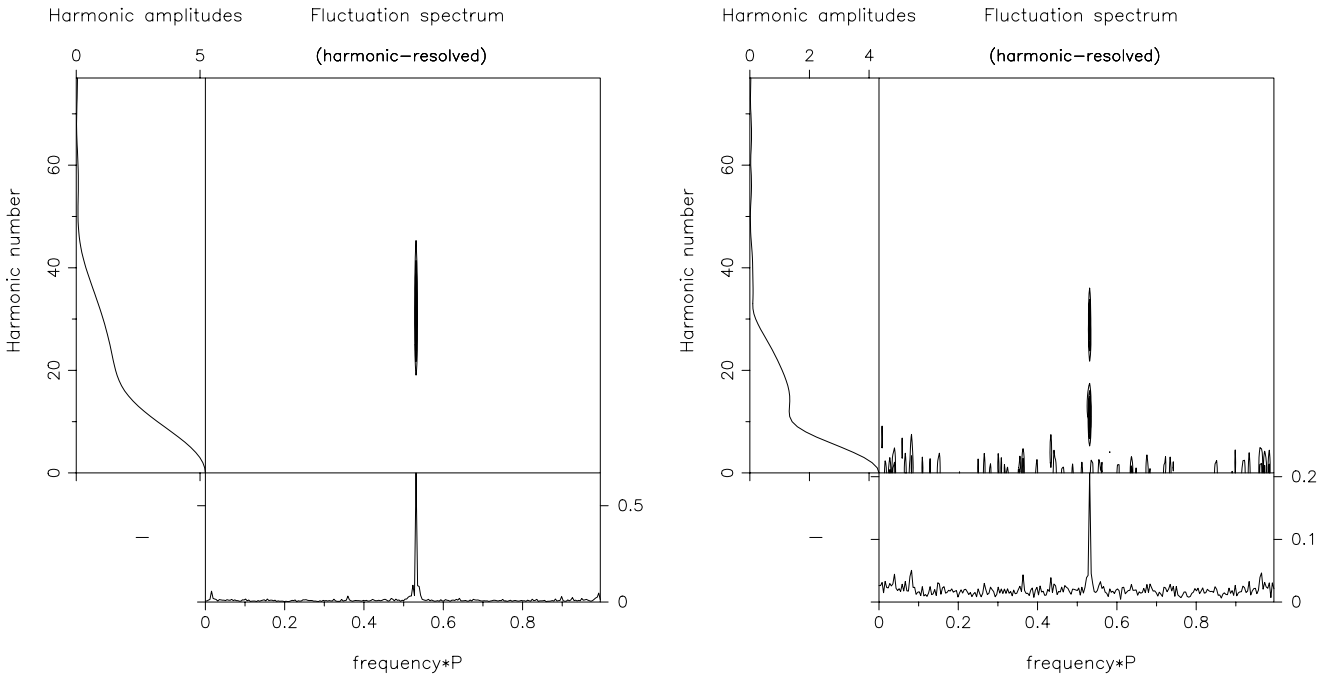


Figure 2. ‘B’-mode HRF spectra for pulsar B0943 + 10 on 1990 December 23 at 103 (left) and 40 MHz (right). These continuously sampled spectra resolve the aliasing of the pulsar’s primary modulation feature, which we now see at about $0.54 c/P_1$. Note also that the feature widths here are narrower, indeed barely resolved. See fig. 4 of Paper I for a complete description.

generally with a reduced precision. We then computed HRF spectra – using overlapping fast Fourier transforms (FFTs) of length 256 wherever possible – for appropriate sections of each ‘B’-mode observation and then interpolated between adjacent Fourier amplitudes to estimate the frequency of the feature and its errors. Examples of

the HRF spectra are displayed in Fig. 2. We see in Table 1 that eight of the 11 dual-band observations are entirely ‘B’-mode sequences and that the end of the first day (December 7) is as well, though its brevity has limited the precision of the values determined. The resulting feature frequencies are tabulated in the column headed f_3

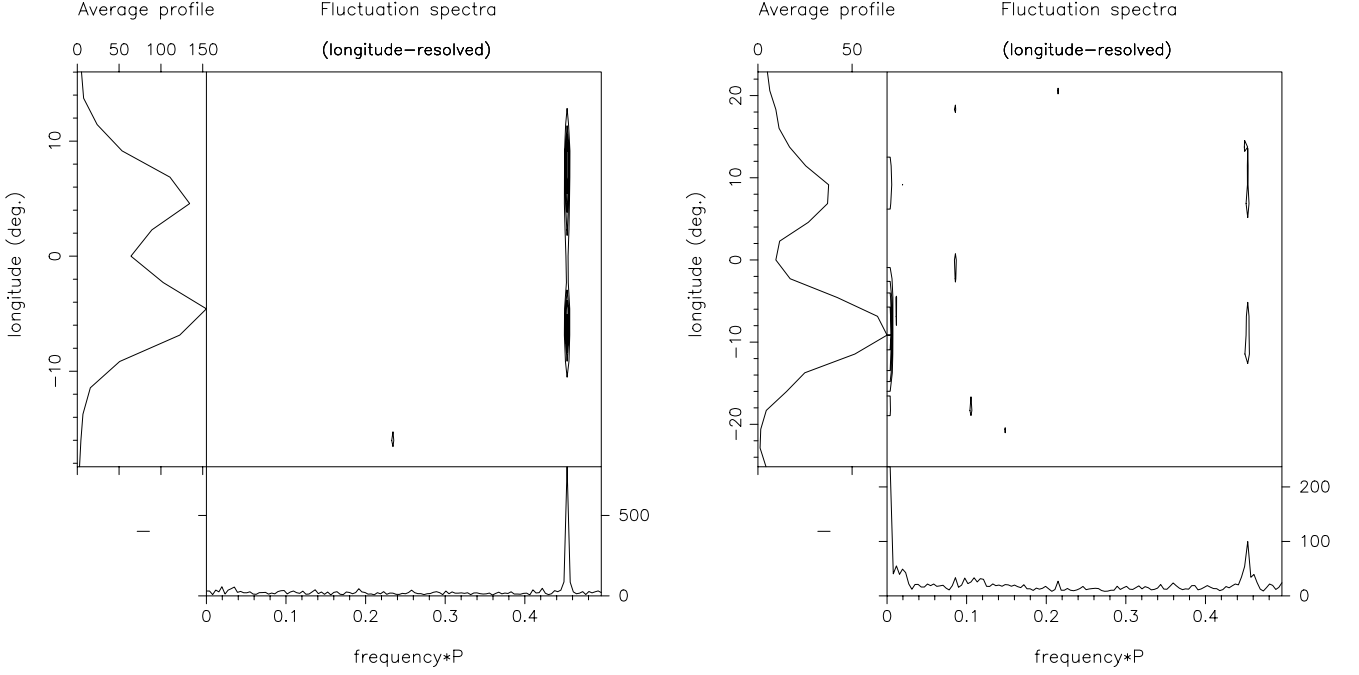


Figure 3. Unusual 'B'-mode profiles and LRF spectra on 1990 December 26 at 103 (left) and 40 MHz (right) as in Fig. 1.

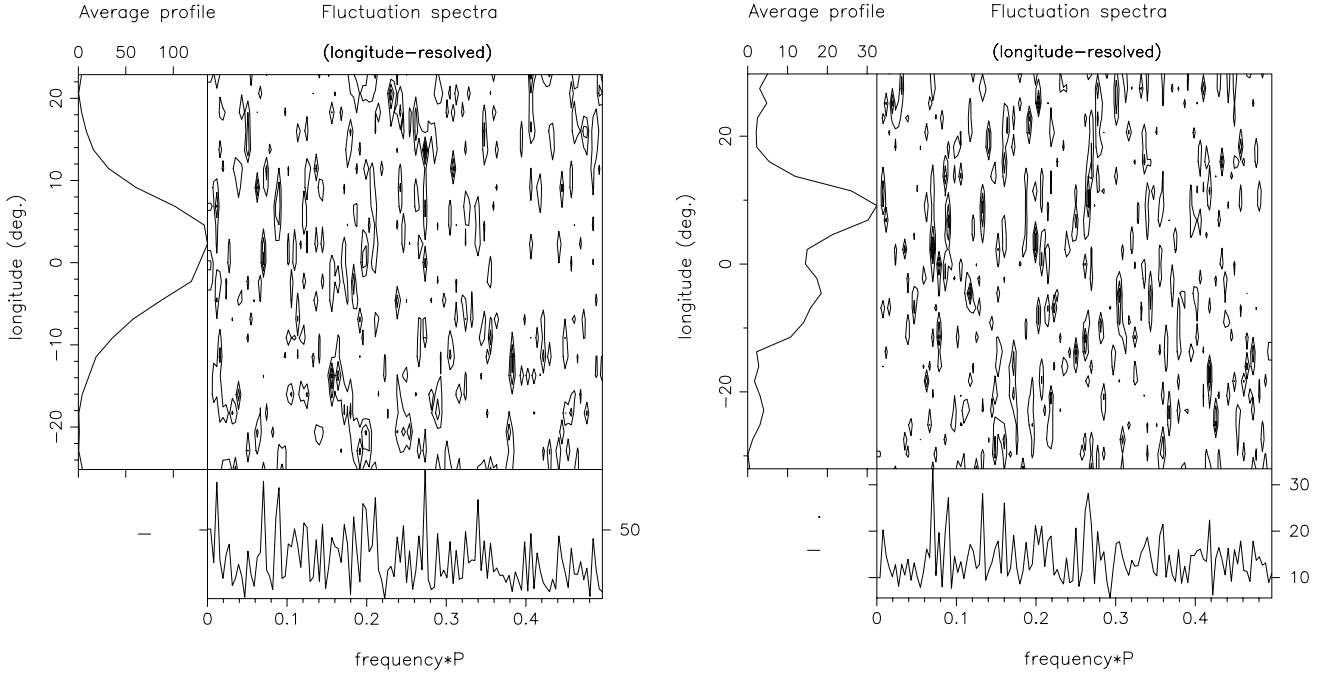


Figure 4. Characteristic 'Q'-mode profiles and LRF spectra on 1990 December 28 at 103 (left) and 40 MHz (right) as in Fig. 1.

and the circulation times in the one labelled \hat{P}_3 ; the errors for both reflect the narrowness of the HRF feature and represent about two standard deviations.

Several interesting results seem to follow from Table 1. First, feature frequencies and circulation times of two different sorts occur among the observations. Most days exhibit f_3 values just over $0.53 c/P_1$ and consequently \hat{P}_3 values well over $37 P_1$ (with many near $37.7 P_1$). However, other days have f_3 values over $0.54 c/P_1$ and thus tertiary modulation periods under 37 periods – indeed, several

around $36.5 P_1$. It is notable that both the first sequence (December 7) – where the short 'B'-mode sequence immediately follows a transition from the 'Q' mode – and the fifth (December 26), whose unusual symmetric profile is reminiscent of 'Q'-mode forms, fall into this latter group. Further study yields the result that the \hat{P}_3 values correlate well with the profile forms: (a) those observations with the usual 'B'-mode profiles, wherein the 103-MHz trailing component is much weaker (some 20 per cent) than the leading one (cf. the 103-MHz profile in Fig. 1), all have \hat{P}_3 values over 37 periods;

Table 1. Properties of the observations.

Date	ν (MHz)	Mode	Good pulse numbers	HRF pulse numbers	MAP pulse numbers	f_3^a (c/P_1)	\hat{P}_3^b (P_1)	$\langle L \rangle / \langle I \rangle^c$ (per cent)
07.12.90	103	Q	34–280	25–280	153–280	–	36.5?	28
	40	Q	34–311	34–311	184–311	–	36.5?	33
	103	B	281–400	273–400	281–400	0.54817 ± 0.00069	36.485 ± 0.046	39
	40	B	312–400	312–400	312–400	0.5535 ± 0.0021	36.13 ± 0.13	39
08.12.90	103	B	145–400	145–400	145–400	0.53574 ± 0.00004	37.332 ± 0.003	25
	40		145–400	145–400	176–400	0.53587 ± 0.00059	37.322 ± 0.041	22
10.12.90	103	B	1–320	193–320	–	0.53108 ± 0.00008	37.659 ± 0.006	46
	40		1–400	1–400	–	0.53085 ± 0.00011	37.675 ± 0.008	38
16.12.90	103	B	2–400	142–397	–	0.54271 ± 0.00005	36.852 ± 0.003	28
	40		1–400	193–320	–	0.54520 ± 0.00020	36.684 ± 0.013	22
17.12.90	103	B	1–400	145–400	145–400	0.53015 ± 0.00003	37.660 ± 0.002	37
	40		1–100	1–128	1–100	0.53071 ± 0.00040	37.686 ± 0.028	31
20.12.90	103	Q	13–400	81–336	–	–	–	28
	40		13–400	81–336	–	–	–	23
22.12.90	103	Q	13–400	–	–	–	–	26
	40		13–400	–	–	–	–	29
23.12.90	103	B	60–340	81–336	81–336	0.53141 ± 0.00004	37.636 ± 0.003	22
	40		2–400	2–400	112–367	0.53058 ± 0.00012	37.695 ± 0.008	25
24.12.90	103	B	1–400	91–346	–	0.54238 ± 0.00003	36.875 ± 0.002	22
	40		1–400	1–400	–	0.54164 ± 0.00036	36.925 ± 0.025	30
26.12.90	103	B	60–340	91–346	91–346	0.54686 ± 0.00003	36.572 ± 0.002	20
	40		1–400	1–400	122–377	0.54738 ± 0.00010	36.538 ± 0.007	20
27.12.90	103	B	80–360	91–346	91–346	0.53234 ± 0.00003	37.570 ± 0.002	25
	40		1–400	1–400	122–377	0.53133 ± 0.00020	37.641 ± 0.014	30
28.12.90	103	Q	100–320	91–346	91–346	–	36.5?	16
	40		2–400	1–400	122–377	–	36.5?	17
11.02.91	103	Q	1–250	1–250	–	–	–	26
13.02.91	103	B	1–250	1–250	–	0.52788 ± 0.00003	37.887 ± 0.022	40
15.02.91	103	Q	1–250	1–250	–	–	–	14
23.01.92	103	B	2–400	81–336	–	0.53101 ± 0.00002	37.664 ± 0.014	70

^aThe tabulated f_3 values refer to the interpolated centroids of the various spectral features (see text), and the error bars indicate the formal (1σ) uncertainties in their estimation (and are thus not the feature widths).

^bThe \hat{P}_3 values are not independently determined, but are computed as $20/f_3$.

^cThe 103-MHz $\langle L \rangle / \langle I \rangle$ values in the last column appear bold and the Q-mode values in italics, respectively, in order to facilitate comparison.

whereas (b) the other PSs with unusual ‘B’-mode profiles, where the 103-MHz trailing component is 50 per cent or more as intense as the leading one (i.e. Fig. 3), all have \hat{P}_3 values under $37 P_1$. These unusual, more symmetrical ‘B’-mode profiles are reminiscent of the symmetrical ‘Q’-mode forms.

It is also worth noting that a range of f_3 values were found in Paper I (see Table 1), although they then did not fall into any discernible pattern. Now we can see that, of the five observations, only the 430-MHz PS from 1972 has an f_3 value that corresponds to a \hat{P}_3 under $37 P_1$, and here only just under. None the less, we find that its profile [not shown here; see fig. 4 in Backer, Rankin & Campbell (1975)] is wider and more symmetric about the longitude of the magnetic axis than its 1992 counterpart.

The ‘B’-mode sequences exhibit a highly ‘coherent’ modulation, and therefore the modulation frequencies and circulation times associated with some of them can be determined to a high precision. In reviewing them it is surprising to find that some of the respective 103- and 40-MHz observation pairs exhibit small modulation frequency differences at a level of a few standard deviations. Moreover, these differences appear somewhat orderly: for the sequences with $\hat{P}_3 \geq 36.9 P_1$, the 40-MHz \hat{P}_3 value is equal to or a little longer than its 103-MHz counterpart; for those more ‘Q’-like sequences with \hat{P}_3 values under $36.9 P_1$, we find an apparent opposite behaviour. Of course, the numbers here are small, and sources of the errors uncertain – indeed, we might attribute a part of the differential to random

changes in the average sub-beam spacing – however, the ostensible order in the values bears further study as longer, higher-quality PS pairs become available.

4 MAPPING THE 103/40-MHZ ‘B’-MODE BEAM STRUCTURE

With this preliminary analysis completed, we are now in a position to construct the sub-beam maps using the ‘cartographic’ transformation discussed in Paper I (see equations 5–8). In addition to the circulation time \hat{P}_3 and the central longitude, this transformation requires as inputs a full specification of the observing geometry – entailing not only the usual magnetic latitude α and impact angle β (determined in Paper I to be 11.6° and -4.31° , respectively⁴) but also

⁴The results of Mitra & Rankin (2002) argue that we observe an outer cone in 0943 + 10, because inner cones seem to have virtually no radial increase at low frequency and thus cannot produce the evolution towards double profile forms seen there. An inner traverse, outer cone model gives α and β values of some 15.4° and -5.69° , respectively. The cartographic transform, however, depends sensitively only on the ratio of these quantities – the PA sweep rate – so that maps using the inner versus outer cone geometry will be virtually indistinguishable apart from their overall angular size. We have thus retained the inner cone model values here, so that the maps of all three papers can be compared directly.

our finding that the sub-beam system rotates anticlockwise around the ‘emitting’ magnetic axis, whereas the star revolves clockwise with respect to the ‘nearer’ rotation axis. Further, in order to ensure that our maps display the same pulses at the same positions for the two frequencies, we took the pulse number origin (k_0 in Paper I, equation 6) to be 31 larger at 40 MHz.

The 103-MHz sub-beam maps divide into three different sorts. First, we have observations in which most of the 20 sub-beams have roughly comparable intensities, the few others being weaker but not absent. This is apparently one of the usual ‘B’-mode configurations, represented well by the December 17 and 23 observations, and a polar map of the latter is given as an example in Fig. 5 (left). Secondly, we see intervals in which several sub-beams are much brighter than the others, dominating the pattern – though again, each of the 20 can be discerned. Examples of this kind occur on December 7, 8 and 26, and Fig. 6 (left) shows this latter behaviour. Finally, we find observations in which the sub-beam intensity is enhanced asymmetrically in one half of the pattern. Our December 27 observation gives such an instance, which is shown in Fig. 7 (left). Note that the presentation of the 103- and 40-MHz maps is slightly different. At 103 MHz, where the ‘base’ (i.e. azimuthal minimum) is well defined, we have subtracted it from the maps in the central panels before plotting; we found, however, that the 40-MHz maps were clearer without this ‘base’ removed.

In the first case – those PSs with rather little variation in their 103-MHz sub-beam intensities – the corresponding 40-MHz maps bear little resemblance to their higher-frequency counterparts. All three such days exhibit much more disordered, ‘patchy’ or asymmetric sub-beam configurations with many sub-beams hardly discernible – though the 20-fold character of the sub-beam pattern is still very strongly maintained. The map of the December 23 sequence in Fig. 5 (right) exhibits both the disorderly character of the 40-MHz pattern and its strong asymmetry. Only the four sub-beams at the top of the diagram and the two on the right are at all prominent; most others are much weaker and some are nearly absent. It is difficult to assess the correspondence between the 103- and 40-MHz patterns. The strong asymmetry in the lower-frequency pattern is not at all apparent in the higher-frequency one – at any orientation. Little more can be gleaned from the December 17 sequence; the 40-MHz pattern is again asymmetric – as perhaps is the higher-frequency one – but at different orientations. In any case, the usable portion of the 40-MHz sequence precedes that at 103 MHz, so they cannot be compared strictly (see Table 1).

Very similar comments can be made for the pair of maps in Fig. 6. Few, if any, of the several brightest beams at 103 MHz are particularly bright at 40 MHz, though the lower-frequency pattern does show several particularly bright sub-beams. Here we might describe the 40-MHz pattern as more ‘patchy’ than asymmetric. Two sub-beams at 40 MHz dominate the pattern, and the corresponding beams at the higher frequency are not especially bright. Nearly identical comments can be made for the December 8 patterns. The December 7 one, however, though shorter, is interesting because it immediately follows a ‘Q’-mode sequence. Here, both patterns are dominated by a few bright sub-beams, and little or no emission can be detected at the positions of others.

The somewhat asymmetric pattern in Fig. 7 provides the most interesting apparent correspondence between the patterns at the two frequencies. The 103-MHz map exhibits a pattern with most of the bright sub-beams at the top left of the map; whereas the 40-MHz pattern also has its brightest sub-beams at the top left of the pattern (as well as a few weaker ones at the bottom). Indeed, a series of six bright sub-beams at the upper left of both patterns are among the

very brightest in both maps. Here, finally, we see what may be an actual correspondence between the patterns at the two frequencies – and at the same orientation.

5 THE 103/40 -MHZ ‘Q’-MODE BEAM STRUCTURE

The one fully ‘Q’-mode observation in Table 1 (December 28) requires little discussion. As is not unexpected, both the 103- and 40-MHz recordings are quite weak; none the less, they represent some of the best such sequences in the Pushchino archive and were consequently chosen to provide a basis for the ‘Q’-mode analysis and discussion in Suleymanova et al. (1998). Polar maps of these data were constructed (not reproduced here), using a nominal value of the circulation time ($36.5 P_1$), and they exhibit no discernible correspondence whatsoever. The top of the 103-MHz map shows two weak inner edge features at about ‘10:45’ and ‘1 o’clock’, while its 40-MHz pair exhibits emission centres at larger radii (or heights) – the brightest squarely at ‘noon’. So, these two maps seem to differ in every possible manner: the patterns are wholly different at the two frequencies, and no rotation would help them to coincide. Moreover, the emission at both frequencies appears to come from somewhat different radii; that at 103 MHz shows a sharp inner edge boundary as if cut off by the sightline traverse (just as we usually see at 430 MHz), while the 40-MHz pattern has a broader radial profile, though peaking at about the same value of some 4.7° [cf. the bottom panels of Figs 5–7 (right)]. In short, our maps of this ‘Q’-mode sequence seem utterly chaotic. It is important to remember that our $36.5 P_1$ circulation-time value is only an estimate, though the PS is so short that this is not very critical.

The beginning of the first observation on December 7 gives us the opportunity to examine the very end of a ‘Q’-mode sequence, when perhaps the emission elements needed for the ‘B’-mode sequence are being re-established. Then, we can estimate the circulation time using the short ‘B’-mode sequence beyond it, which we noted above was about $36.5 P_1$ – and even if this is in error, we have a sequence of only about four times this length to map. It is worth mentioning that we see no hint of the primary modulation feature in these ‘Q’-mode sequences, which is perhaps their primary defining feature.

The respective 103- and 40-MHz maps for these ‘Q’-mode sequences in Fig. 8 appear to show more correspondence than any we have examined thus far – though the S/N is poor owing to the weakness and shortness of the sequence, so careful inspection is required. In both, we find a strip of emission on the bottom inner edge of the pattern – and especially between about ‘4:30’ and ‘8:30’ – which appears to continue around to ‘noon’ or ‘1 o’clock’. In both, the weakest and least orderly part of the pattern is between about ‘1:30’ and ‘4:30’. Some features in the middle and outer parts of the patterns may also correspond; note particularly the bright outer edge feature at about ‘4:30’. However, the inner edge regions between about ‘4:30’ and ‘8:30’ are especially interesting. The higher-frequency map indeed shows what appears to be a fairly regular series of some eight weak ‘beamlets’ over this 120° section of the map, and while the resolution of the 40-MHz map is poorer, a number of comparable features are seen here around its radial maximum.

Though we can only speculate about the significance of these weak and noisy patterns (weakness again being one of the usual characteristics of the ‘Q’ mode), these maps represent our first opportunity to examine a ‘Q’-mode sequence which immediately precedes a transition to the ‘B’ mode. Here, indeed, we are examining the final 128 such pulses, prior to the abrupt ‘B’-mode onset at pulse 281/312. Does the ‘4:30’ feature represent one of the last

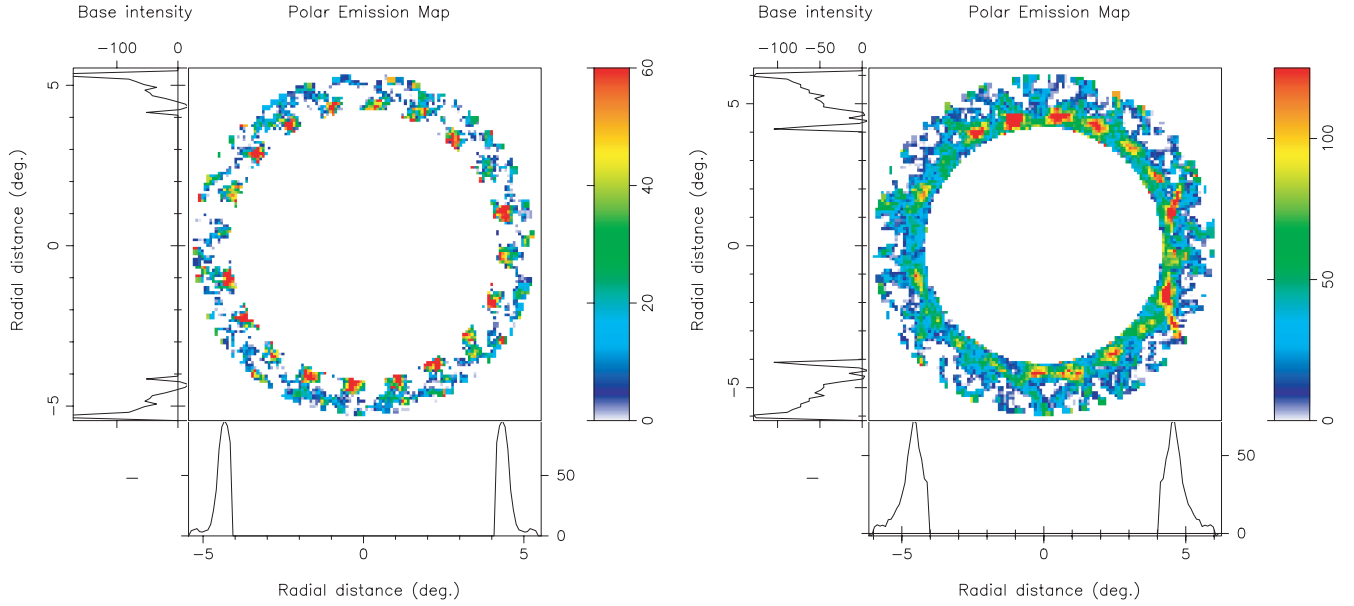


Figure 5. ‘B’-mode polar maps for pulsar B0943 + 10 on 1990 December 23 at 103 (left) and 40 MHz (right). These images reflect fully simultaneous sequences of 256 pulses. The polar map is projected on to the polar cap shown in the main panel, with the ‘closer’ rotational axis at the top of the diagram. The star rotates clockwise, causing the sightline to cut the anticlockwise-rotating sub-beam system from left to right. The bottom and the side panels show the average and the ‘base’ intensity profiles, respectively, as functions of the angular distance from the magnetic axis. The 103-MHz ‘base’ has been subtracted from the pattern in the central panel, whereas the 40-MHz ‘base’ has not. The 103-MHz map is a good example of those in which most of the sub-beams have roughly uniform intensity. Note the track of one unusually bright pulse at the right of the 40-MHz map.

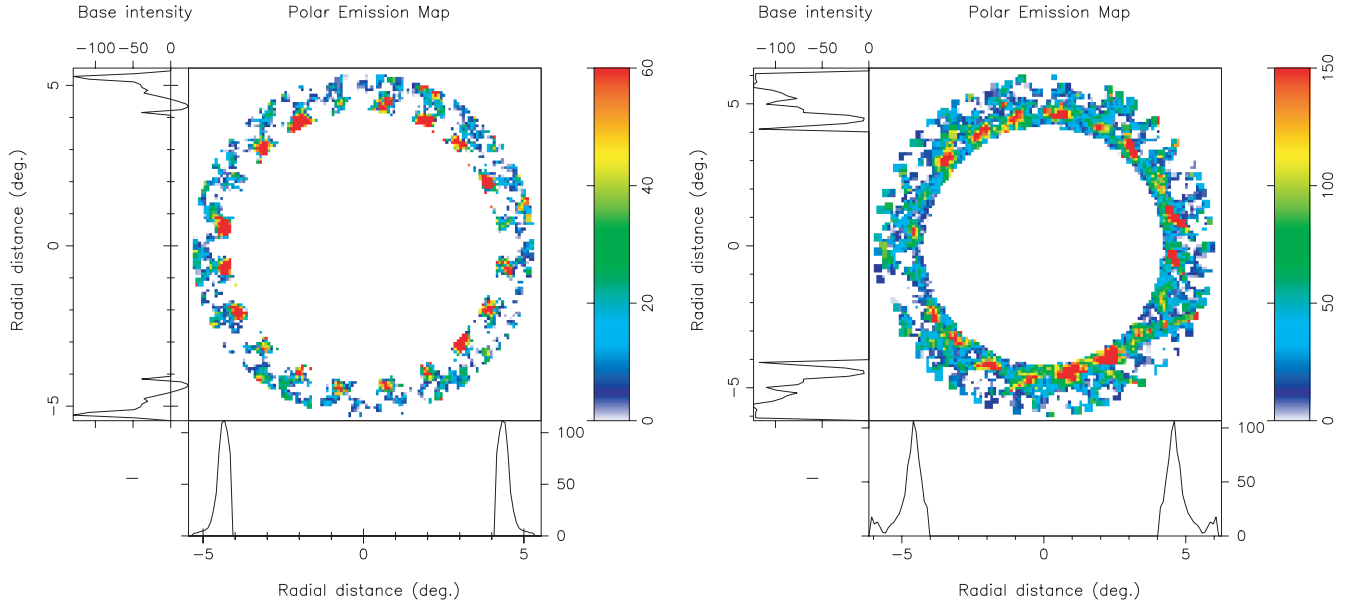


Figure 6. ‘B’-mode polar maps on 1990 December 26 at 103 (left) and 40 MHz (right) as in Fig. 5. This 103-MHz map is a good example of those in which a few sub-beams tend to dominate the others.

‘Q’-mode sub-beams, emitting here characteristically at a larger radius or height? Also, does the system of weak, inner edge ‘beamlets’ represent the reformation of the vigesimal ‘B’-mode configuration? Note that these are too narrowly spaced, eight in 120° or 24 overall, to generate the usual ‘B’-mode modulation. Indeed, one can imagine that there are a total of about 20 such ‘beamlets’ around the inner edge of the pattern at 103 MHz, but, apart from the ‘4:30-to-8:30’ group, they lie at discernibly irregular intervals. (It is also worth noting that ‘B’-mode maps, constructed from the first 100 or so pulses

following the transition, bear no resemblance to the ‘last’ ‘Q’-mode maps we are examining here.)

Lastly, note that the emission in both ‘Q’-mode patterns is on their leading edges. We see radial profiles that are truncated at the sightline impact angle β , not peaking well outside it as in all the other ‘B’-mode maps encountered earlier. However seriously we take the above interpretation of the maps in Fig. 8, it does not begin to fully elucidate what electrodynamic conditions change so abruptly to re-establish the ‘B’-mode patterns. In the space of one stellar rotation,

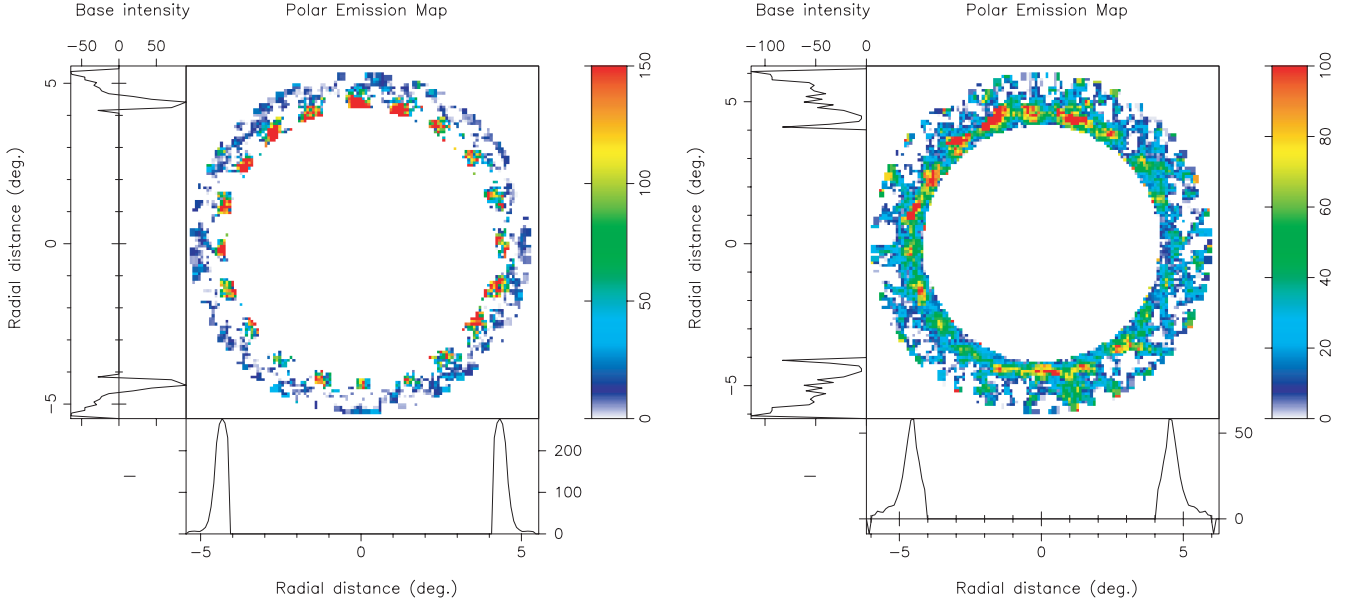


Figure 7. 'B'-mode polar maps on 1990 December 27 at 103 (left) and 40 MHz (right) as in Fig. 5. This 103-MHz map is a good example of those in which the sub-beams assume an antisymmetric distribution about the magnetic axis.

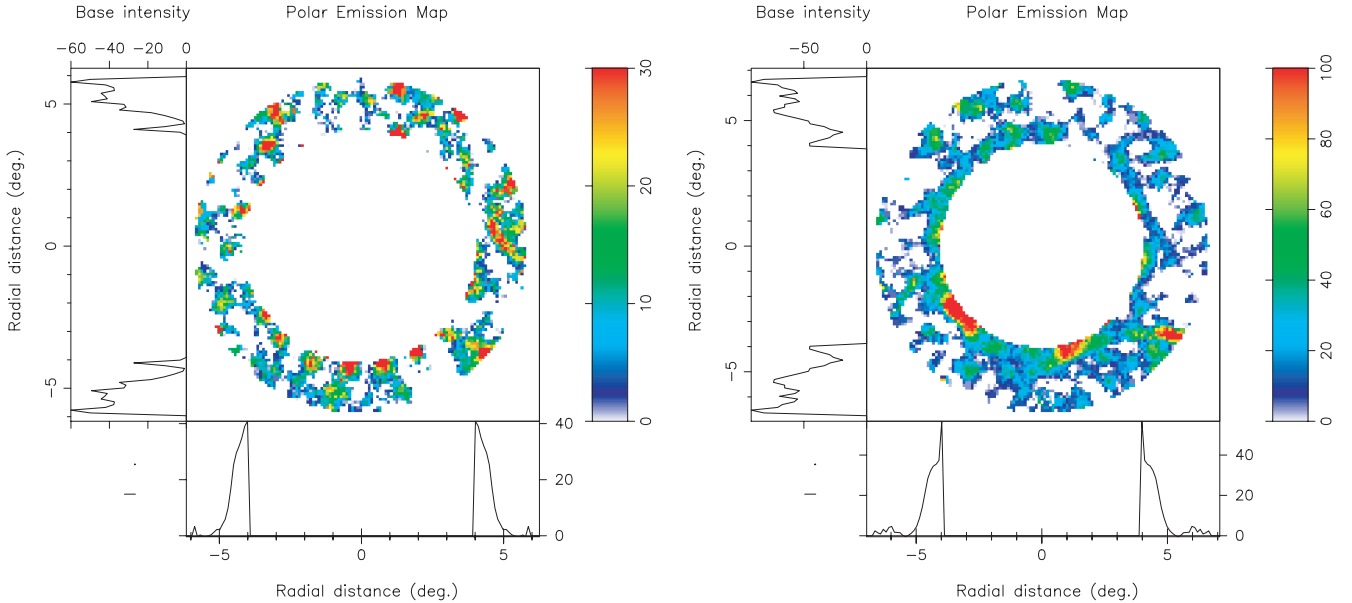


Figure 8. 'Q'-mode polar maps on 1990 December 7 at 103 (left) and 40 MHz (right). These polar maps (as in Fig. 5) correspond to the last 128 pulses before the onset of the 'B' mode. They have been smoothed by a circular function 0.06° in diameter to improve the S/N.

not only does the strict, 20-fold sub-beam pattern reassert itself, but the gross distribution of emission changes from one which is roughly symmetrical about the longitude origin (that of the magnetic axis) to one asymmetrically favouring earlier longitudes. Of course, we can readily note this abrupt change both in the raw sequences as well as in the different forms of the 'B'- and 'Q'-mode profiles – though we also now know from Suleymanova et al. (1998) that slow variations precede 'B'- to 'Q'-mode changes. We will see below a variety of 'B'-mode polarization characteristics.

6 POLARIZATION MODE BEHAVIOUR

Linear polarization information was available for all of the sequences, following the Faraday modulation technique described

above. On this basis it was possible to study the average profile polarization and PA traverse as had been done earlier by Suleymanova et al. (1998). The quality of the various observations was quite uneven – though in all cases it was possible to measure or estimate the mean fractional linear polarization to better than about 5 per cent. These latter values are given in the right-most column of Table 1, and the 103-MHz and Q-mode entries are shown in boldface and italics, respectively, to make comparison easier. The four highest-quality 'B'-mode sequences, those on 1990 December 23, 1990 December 27, 1991 February 13 and 1992 January 23, are nearly equal in overall S/N, but vary markedly in average linear polarization: the first two have only 20–25 per cent linear polarization, while the last two have some 40 and about 70 per cent, respectively. The remaining 103-MHz 'B'-mode PSs all fall within this range,

whereas the 103-MHz ‘Q’-mode profiles consistently exhibit depolarized profiles with fractional linear polarization less than 25 per cent. Finally, the polarization estimates for the 40-MHz profiles suggest that the fractional linear polarization variations correlate well with the higher frequency; we computed a correlation coefficient of some 60 per cent.

Overall, a much larger proportion of the total samples at the higher frequency were strong enough to give a reliable estimate of the linear Stokes parameters Q and U , and only for one of these – the 103-MHz sequence on 1990 December 23 – was a significant proportion of secondary polarization mode (SPM) samples detected. Among the four best ‘B’-mode PSs mentioned above, the fractional linear polarization variations are anticorrelated with the number of SPM-dominated samples detected. In PA histograms we see clear ‘patches’ of SPM emission in the first two least linearly polarized PSs, less in the 1991 PS, and no clear SPM emission at all in the last, most highly polarized observation.

It happened that most of the SPM samples in the 1990 December 23 PS represented negative values of Stokes Q (such that little power was in Stokes U), so a polar map in this quantity (not shown) was computed and inspected. While it suggested a modal sub-beam configuration much like that of the 430-MHz map in Paper I (their fig. 19), unfortunately here also the SPM-dominated samples did not carry a very large fraction of the fluctuating power, so they were not easy to distinguish from the noise power in the map.

In a further effort to understand the modal character and variations of profile polarization, we computed sets of partial profiles corresponding to progressive quarter phases of the $1.87\text{-}P_1$ modulation cycle – just as we did earlier in Paper I (their fig. 6) for the 430-MHz observation. An example for 1990 December 27 is given in the six panels of Fig. 9, but similar analyses were carried out for the other three best ‘B’-mode sequences above. The four left-most panels give the partial profiles at 90° modulation phase intervals, and the ‘drift’ can be seen as a cyclical motion of the (mean) sub-pulses from right to left, some 3° longitude from panel to panel. The top- and bottom-right panels then show the forms of the mean ‘drifter’ and ‘base’, respectively. Overall, the displays depict the behaviour of the primary polarization mode (PPM), as can be seen clearly in the ‘drifter’, although the slight residual polarization of the ‘base’ is nearly orthogonal. Note, however, that the (mean) sub-pulses are highly polarized apart from some of their edges, where the depolarization can be seen clearly. Here, indirectly, we are probably seeing the effects of the SPM, and some abrupt rotations of the PA (cf. panel b) further suggest near SPM dominance at these points.

Despite these detailed analyses, it is not entirely clear just what changes to produce the very great variations in ‘B’-mode aggregate linear polarization. The origin of the non-drifting ‘base’ emission is key to this understanding as it is necessarily defined by its total intensity but can accumulate as a result of the depolarization. Overall, the subpulse polarization is very high, often appearing to reach 100 per cent. SPM-associated depolarization is very clear in the first two sequences, discernible in the third, but not so in the last observation. It would thus appear that changes in the modal configuration of the rotating sub-beam system are required to produce the observed variations in the fractional linear polarization – indeed, that the ratio of PPM to SPM power changes, but also that its angular offsets (and thus consequent depolarization characteristics) vary somewhat. Future observations with both better resolution and better S/N will be needed to untangle these complicated effects.

7 SUMMARY AND DISCUSSION

Above, we have studied observations of pulsar 0943 + 10, using mostly simultaneous 103- and 40-MHz sequences from the Pushchino Observatory. Eight of the observations were ‘B’-mode sequences, three were ‘Q’-mode observations, and a further recorded a ‘Q’- to ‘B’-mode transition.

Our main results can be summarized as follows:

(i) The measured P_3 and \hat{P}_3 values for the five ‘normal’ ‘B’-mode sequences fall within a narrow range just over $0.54 c/P_1$ and around $37.7 P_1$, respectively. Four other ‘B’-mode sequences, one immediately following a ‘Q’-mode sequence and another with an unusual symmetrical (‘Q’-mode-like) 103-MHz profile, have P_3 s well over $0.54 c/P_1$ and \hat{P}_3 values around $36.5 P_1$. Perhaps, these latter circulation times pertain more to what occurs during ‘Q’-mode sequences.

(ii) Of these nine ‘B’-mode PSs, the ‘normal’ ones all have a weakish second component, while all of the ‘Q’-mode-like ones show an accentuated (or more symmetrical) second component.

(iii) In most cases the 103- and 40-MHz PS pairs exhibit small differences in circulation time \hat{P}_3 . These differences represent only a few standard deviations in the errors, and such discrepancies could arise from random causes (i.e. small differences in mean sub-beam spacing). However, the behaviour appears orderly and suggests a slightly slower relative 40-MHz rotation for the ‘normal’ ‘B’-mode sequences and a faster rotation of the ‘Q’-mode-like ones.

(iv) Maps of the Pushchino 103-MHz ‘B’-mode sequences do not look very different from the Arecibo 111-MHz recording analysed in Paper I (their fig. 26). However, six such sequences were here available for study. All exhibited the characteristic 20-fold sub-beam pattern [see Figs 5–7 (left)]. In some all 20 sub-beams had comparable intensities, while in others one or two sub-beams were exceptionally bright. Finally, one had what appears to be a partially developed antisymmetric pattern with most of the emission on one ‘side’ of the pattern.

(v) Similarly, many of the Pushchino 40-MHz ‘B’-mode sequences look very much like the 35-MHz maps of the Gauribidanur observations in Paper II. However, here we can see that even as uniform a pattern as that of the G observation in Paper II (their fig. 7) is quite unusual. Most of our observations result in maps more like the C series in Paper II (their fig. 6), with however perhaps even more corrugation of the sub-beam intensity.

(vi) We cannot know whether any correspondence between the systems of sub-beam intensities at two frequencies would occur without a rotation between the patterns, so we have been open to this possibility. Generally, we have found very little discernible correspondence between the 103- and 40-MHz ‘B’-mode map pairs; indeed, for five of the six patterns, almost none. The single ‘B’-mode observation which exhibits an apparent correspondence is the December 27 sequence depicted in Fig. 7, and, if actual, the maps correspond without any relative rotation.

(vii) Surprisingly, it is a pair of short ‘Q’-mode maps which may show the most correspondence. The December 7 sequence, which represents the first recording of a ‘Q’-mode to ‘B’-mode transition, exhibits corresponding bright and dim regions (without added rotation), particularly near the ‘bottom’, inner edge of the patterns. The 128-pulse sequence in question may indicate a series of up to 20 ‘beamlets’, which are not uniformly spaced in azimuth, within the pattern. Eight of these around the bright bottom edge have regular spacings a little less than the usual 18° ‘B’-mode configuration. It is interesting that the ‘B’-mode sequence which commences

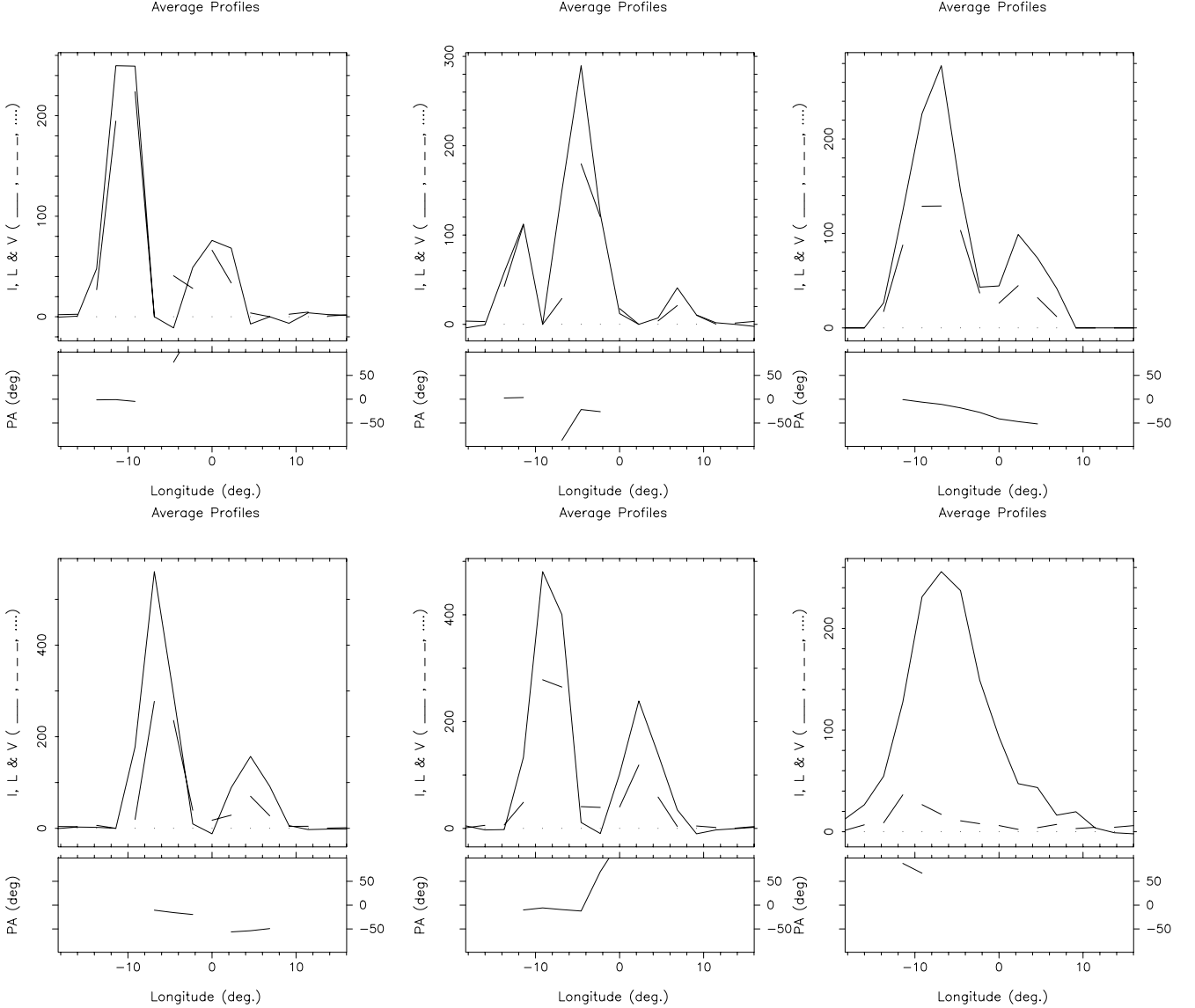


Figure 9. Composite of four partial polarization profiles (left, centre) folded at different phases of the nominal 1.87- P_1 modulation cycle as well as partial profiles of both the ‘drifting’ power (top right) and the ‘base’ (bottom right). All were computed from pulses 91–346 of the 1990 December 27 ‘B’-mode sequence mapped in Fig. 7 (left). Two and at times three subpulses are seen in the four panels which ‘drift’ progressively from later to earlier phases about 3° from plot to plot. Note that their form and amplitude are windowed strongly by the overall double form of the average profile [not shown, but similar to that in the left-hand panel of Fig. 1 (left)]. Stokes V does not exist for these sequences, and thus the dotted curves are uniformly zero.

immediately afterwards has a pattern with little or nothing in common with this ‘Q’-mode pattern.

(viii) We confirm the earlier result that ‘B’-mode profiles tend to be more highly polarized than their ‘Q’-mode counterparts and that this results from differing ratios of PPM and SPM power. However, we have found a good deal of variation in the fractional linear polarization of the profiles overall, and these variations appear well correlated between the two frequencies – again providing strong evidence that these are also produced by varying proportions of modal power.

(ix) The 12 observations reported here were chosen from among a programme of 22 sequences from 1990 December for their good quality at both 103 and 40 MHz. Therefore, the relative occurrence frequency of ‘B’-mode and ‘Q’-mode sequences has been skewed. The ratio first reported by Suleymanova & Izvekova (1984) – about

equal – was confirmed using the full set by Suleymanova et al. (1998).

(x) These PRAO observations, together with those considered in Papers I and II, comprise some 8000 pulses, during which two modal transitions were encountered – one of each type. If ‘B’- and ‘Q’-mode sequences represent a cycle, then we might estimate that its duration is some 2.5 h or so and that ‘B’-mode sequences persist for 1.5 h or some 5000 pulses. It will be interesting, when longer sequences become available, to see how these estimates bear on their reality.

These Pushchino observations give further credence to the picture that subpulse emission takes place in connection with a series of emission columns, which, being ‘seeded’ in the polar cap region near the surface of the star, rise up through the polar flux tube into

the emission zone at a height of several hundred kilometres, and then extend out to much greater distances, perhaps into the ambient medium around the star. The rotation axis of pulsar 0943 + 10 makes only a small angle with its magnetic polar axis, so these emission columns would extend in a direction nearly parallel to the rotation axis (or along the centre of the velocity-of-light cylinder). The stable ‘B’-mode system is configured of just 20 such columns, whose integrity we have seen maintained throughout the range of emission heights sampled by our various observations. We do see, however, a progressive disordering of the sub-beam configuration – little between 430 and 111 MHz, but perceptibly more at 35 and 40 MHz. Using the model of Paper I (their table 2), the former lie within about 15 km of each other at 131 and 147 km, whereas the latter are some 30 km further away at some 170 km.⁵

During the ‘B’-mode sequences, we might speculate that this system of emission columns undergoes a progressive twisting by the rotating star (recall that its rotation and magnetic axes are closely aligned) – most of it presumably well above the emission regions where the magnetic field weakens sufficiently. We might then expect that there is some physical maximum to the amount of distortion this system of emission columns can sustain, and that exceeding this maximum produces an unstable, much simpler, emission beam configuration which we know as that of the ‘Q’ mode. During these sequences, emission may be excited along some of these same columns, but in the dramatic, but disorganized, manner characteristic of the ‘Q’ mode. Then, after some time, when the emission column distortion has had a chance to recover, another stable ‘B’-mode configuration can be reinstated.

While features of this overall picture may describe the physical conditions producing the modal sequences of 0943 + 10, including both the near-instantaneous ‘snap’ transitions at the modal boundaries as well as the slow changes in intensity and profile form which were identified by Suleymanova et al. (1998), other aspects of the modal changes remain unclear. To wit, the ‘B’-mode emission distribution is characteristically asymmetric about the longitude of the magnetic axis – or, what is the same, their profiles usually show most of the power at negative longitudes – whereas ‘Q’-mode power is either roughly symmetric or even favouring of trailing longitudes. Given our now clear understanding that the sub-beam rotation is continuous – and thereby symmetrical about the magnetic axis – these asymmetries, along with their both slow and rapid variations, assume a new significance.

⁵The outer cone model heights for 430, 111/103 and 35/40 MHz are 231, 261 and 300 km, respectively. See Mitra & Rankin (2002) for more physical height values corresponding to these model computations.

Physically, the remarkable coherence of this pulsar’s sub-beam patterns over the entire frequency range for which pulse-sequence observations are possible – nearly four octaves – points strongly to an $\mathbf{E} \times \mathbf{B}$ drift mechanism as first suggested by Ruderman & Sutherland (1975). Whether, however, this model’s other physical expectations (including that the primary particle acceleration occurs just above the magnetic polar cap) remain an open, but now actively debated, question (e.g. Asseo & Khechinashvili 2002; Gil, Melichidze & Mitra 2002; Wright 2002).

This all said, we see that pulsar B0943 + 10, having been the agency of considerable new knowledge about its conditions of emission, still has a great deal to teach us. Studies of long sequences – which continuously encounter a few mode changes – should provide answers to some of the questions above. New and better polarimetry will also provide new insights, as will study of other pulsars with both similar and dissimilar properties.

ACKNOWLEDGMENTS

It is a pleasure to thank both Slava Pugachev for assistance in developing programs used in the observations and analysis, and Geoff Wright for his critical comments on the paper in draft. One of us (JMR) also wishes to acknowledge the hospitality of the Raman Research Institute where this work was initiated. This work was also supported in part by US NSF Grants AST 99-86754 and 00-98685 as well as under a Visitor Grant from the Nederlandse Organisatie voor Wetenschappelijk Onderzoek.

REFERENCES

- Asgekar A. A., Deshpande A. A., 2001, MNRAS, 326, 1249 (Paper II)
 Asseo E., Khechinashvili D., 2002, MNRAS, 334, 743
 Backer D. C., Rankin J. M., Campbell D. C., 1975, ApJ, 197, 481
 Deshpande A. A., 2000, in Kramer M., Wex N., Wielebinski R., eds, ASP Conf. Ser. Vol. 202, Pulsar Astronomy–2000 And Beyond (IAU Colloq. 177). Astron. Soc. Pac., San Francisco, p. 149
 Deshpande A. A., Rankin J. M., 1999, ApJ, 524, 1008
 Deshpande A. A., Rankin J. M., 2001, MNRAS, 322, 438 (Paper I)
 Gil J. A., Melichidze G. I., Mitra D., 2002, A&A, 388, 246
 Mitra D., Rankin J. M., 2002, ApJ, 577, 322
 Rankin J. M., Deshpande A. A., 2000, in Kramer M., Wex N., Wielebinski R., eds, ASP Conf. Ser. Vol. 202, Pulsar Astronomy–2000 And Beyond (IAU Colloq. 177). Astron. Soc. Pac., San Francisco, p. 155
 Ruderman M. A., Sutherland P. G., 1975, ApJ, 196, 51
 Suleymanova S. A., Izvekova V. A., 1984, SvA, 28, 53
 Suleymanova S. A., Volodin Yu. V., Shitov Yu. P., 1988, AZh, 65, 349
 Suleymanova S. A., Izvekova V. A., Rankin J. M., Rathnasree N., 1998, JA&A, 19, 1
 Wright G. A. E., 2002, MNRAS, submitted

This paper has been typeset from a $\text{\TeX}/\text{\LaTeX}$ file prepared by the author.